

Near-infrared integral-field spectra of the planet/brown dwarf companion AB Pictoris b^{*}

M. Bonnefoy¹, G. Chauvin¹, P. Rojo², F. Allard³, A.-M. Lagrange¹, D. Homeier⁴, C. Dumas⁵, and J.-L. Beuzit¹

¹ Laboratoire d'Astrophysique, Observatoire de Grenoble, 414 rue de la piscine, 38400 Saint-Martin d'Hères, France
e-mail: mbonnefo@obs.ujf-grenoble.fr

² Departamento de Astronomia, Universidad de Chile, Casilla 36-D, Santiago, Chile

³ CRAL-ENS, 46, Allée d'Italie, 69364 Lyon Cedex 07, France

⁴ Institut für Astrophysik Göttingen, Georg-August-Universität, Friedrich-Hund-Platz 1, 37077 Göttingen, Germany

⁵ European Southern Observatory, Casilla 19001, Santiago 19, Chile

Received 12 June 2000 / Accepted 22 December 2009

ABSTRACT

Context. We have already imaged a co-moving companion at a projected separation of ~ 260 AU from the young star AB Pic A. Evolutionary model predictions based on *JHK* photometry of AB Pic b suggest a mass of $\sim 13\text{--}14 M_{\text{Jup}}$, placing the object at the deuterium-burning boundary.

Aims. We aim to determine the spectral type, the surface gravity, and the effective temperature of AB Pic b. From the comparison of our absolute photometry to surface fluxes generated by atmospheric models, we also aim at deriving mass and radius estimates that are independent of evolutionary model predictions to test and refine them.

Methods. We used the adaptive-optics-fed integral field spectrograph SINFONI to obtain high-quality, medium-resolution spectra of AB Pic b ($R_{\lambda} = 1500\text{--}2000$) over the $1.1\text{--}2.5 \mu\text{m}$ range. Our analysis relies on comparing our spectra to young standard templates and to the latest libraries of synthetic spectra developed by the Lyon group.

Results. AB Pic b is confirmed as a young early-L dwarf companion. We derive a spectral type L0–L1 and find several features indicative of an intermediate gravity atmosphere. A comparison to synthetic spectra yields $T_{\text{eff}} = 2000^{+100}_{-300}$ K and $\log(g) = 4 \pm 0.5$ dex. Determination of the derived atmospheric parameters of AB Pic b is limited by an imperfect match of current atmosphere spectra with our near-infrared observations of AB Pic b. The current treatment of dust settling and the missing molecular opacity lines in the atmosphere models could be responsible. By combining the observed photometry, the surface fluxes from atmosphere models and the known distance of the system, we derive new mass, luminosity, and radius estimates of AB Pic b. They independently confirm the evolutionary model predictions. We finally review the current methods used for characterizing planetary mass companions and discuss them in the perspective of future planet deep-imaging surveys that will be faced with the same limitations.

Key words. planetary systems – techniques: spectroscopic

1. Introduction

Understanding how planets form and evolve and which physical processes affect their atmospheric chemistry remains a major challenge in exoplanetary science, ever since the first glimpse of planetary formation revealed by the discovery of the β Pictoris star debris disk (Smith & Terrile 1984). Radial-velocity and transit searches have detected more than 300 exoplanets and, in some favorable cases, enabled a spectroscopic characterization of the irradiated atmospheres of transiting giant planets to be initiated (Vidal-Madjar et al. 2004; Tinetti & Beaulieu 2009; Barnes et al. 2009). However, these techniques remain limited to the study of close-in planets with orbital radii typically smaller than 5 AU.

At wider orbits, the deep imaging technique with space telescopes (e.g. HST) or the combination of adaptive optics (AO) systems with very large ground-based telescopes (e.g. Palomar, CFHT, Keck, Gemini, Subaru, VLT) is particularly well-suited. The recent identification of young (≤ 100 Myr), nearby (≤ 100 pc)

stars that are members of comoving groups (Kastner et al. 1997; Zuckerman & Song 2004; Torres et al. 2008) has offered ideal targets to look for substellar companions. Over the past years, several brown dwarf companions have been successfully detected at relatively wide (≥ 40 AU) orbits from their central stars (Lowrance et al. 1999, 2000; Chauvin et al. 2003). The planetary mass companion imaged at ~ 41 AU from the young nearby brown dwarf 2M1207 (Chauvin et al. 2004) finally opened the way to new discoveries of other classes of targets, members of distant open clusters (Itoh et al. 2005; Neuhäuser et al. 2005; Luhman et al. 2006; Lafrenière et al. 2008; Schmidt et al. 2008), and nearby intermediate-age (0.1–1.0 Gyr) stars (Metchev et al. 2006) and to the recent breakthrough discoveries of HR 8799 bcd (Marois et al. 2008b), Fomalhaut b (Kalas et al. 2008), and the β Pic b candidate (Lagrange et al. 2008).

In most cases, the companionship was generally confirmed by follow-up observations to show that the star and its companion share a common proper motion, whereas the companion mass was always assumed from a comparison of the companion photometry with evolutionary model predictions at the system age and distance. In some cases, high-quality spectra have allowed deviation of the companion spectral type to confirm its relatively cool atmosphere by identifying broad molecular

* Based on service-mode observations (080.C-0590(A)) collected at the European Organization for Astronomical Research in the Southern Hemisphere, Chile.

Table 1. Observing log.

UT Date	Target	Grating	R_λ	Pre-optic (mas/pixel)	sec z	$FWHM$ (")	$\langle EC \rangle$ (%)	$\langle \tau_0 \rangle$ (ms)	DIT (s)	NDIT	t_{exp} (s)	Note
05/12/2007	AB Pic b	J	2000	25×12.5	1.225/1.221	1.05/0.81	54.4	60.13	300	1	2700	
05/12/2007	AB Pic b	J	2000	25×12.5	1.199/1.198	0.72/0.83	54.6	71.73	300	1	2700	
05/12/2007	HIP039640	J	2000	25×12.5	1.202/1.200	1.34/1.20	38.9	120.91	40	1	80	Tel STD
11/12/2007	AB Pic b	J	2000	25×12.5	1.199/1.198	0.82/0.81	51.5	66.16	300	1	2700	
11/12/2007	HIP023230	J	2000	25×12.5	1.214/1.218	0.96/1.24	39.5	133.44	60	1	120	Tel STD
12/11/2007	AB Pic b	$H + K$	1500	25×12.5	1.200/1.201	1.67/1.74	14.9	11.15	300	1	2700	
12/11/2007	HIP037963	$H + K$	1500	25×12.5	1.211/1.210	2.32/2.31	05.4	6.11	20	3	120	Tel STD

absorptions. The effective temperature T_{eff} and the surface gravity $\log(g)$ can sometimes be derived using temperature- and gravity-sensitive features (Gorlova et al. 2003; Allers et al. 2007) by comparison to the template spectra of field and young dwarfs (McLean et al. 2003; Cushing et al. 2005; Lodieu et al. 2008) or using atmosphere models. However, systematic and homogeneous photometric and spectroscopic characterization of young wide planetary mass companions are essential for further constraining interior and atmosphere models that could depend on their formation mechanisms (Marley et al. 2007).

In the course of a VLT/NACO deep coronagraphic imaging survey of young, nearby stars (Chauvin et al. 2009), Chauvin et al. (2005a) discovered a faint comoving source at 5.5" (~ 260 AU) from the young star AB Pic A (HIP30034, K2V, $V = 9.16$, $d = 45.5^{+1.8}_{-1.7}$ pc, Perryman et al. 1997). AB Pic A was originally identified as a member of the Tucana-Horologium association (Tuc-Hor) from its distance to the Earth, the strength of the $\lambda 6708$ Li line ($EW = 260 \pm 20$ mÅ; confirmed by Mentuch et al. 2008), its filled-in $H\alpha$ absorption, and the saturated L/L_X emission (Song et al. 2003, hereafter S03). S03 also obtained galactic space motions and found them to be similar to those of newly identified Tuc-Hor members. At the age of the association (~ 30 Myr, see Torres et al. 2000; Stelzer & Neuhäuser 2000; Zuckerman & Webb 2000; Zuckerman et al. 2001; Torres et al. 2001; Scholz et al. 2007; Mentuch et al. 2008), several evolutionary models predict a companion mass of 13–14 M_{Jup} , in agreement with the L0–L3 spectral type derived from NACO K -band spectroscopy. This places AB Pic b at the planetary mass boundary ($\sim 13.6 M_{\text{Jup}}^1$). Recently, Makarov (2007) has claimed that AB Pic b could be a member of the β Pictoris association (β Pic) because of a lower metallicity compared to Tuc-Hor members and a study of mutual conjunctions with the ρ Ophiucus and Upper Sco star-forming regions. The system would be therefore considerably younger. However, this classification must be reconsidered in light of recent Viana Almeida et al. (2009) results assigning a solar metallicity to AB Pic A (Makarov, Private Com.). Alternatively, Torres et al. (2008) classified AB Pic A as a member of the 30 Myr-old Carina association from its enhanced L/L_X emission and a convergence kinematical method described in Torres et al. (2006). In all cases, this membership revision does not modify the age of AB Pic A and b and the conclusion of Chauvin et al. (2005b).

We present here high-quality near-infrared spectra of the AB Pic b companion. They constitute the first results of a homogeneous survey to build an empirical library of carefully processed near-infrared spectra for young very-low mass companions. The observations of AB Pic b and the associated data-reduction are presented in Sect. 2. The analysis of our spectra is presented in Sect. 3. In Sect. 4, we derive new mass, radius, and luminosity estimations using various methods to compare their

respective limitations in the perspective of a future deep-imaging search for giant planets.

2. Observations and data reduction procedures

We used the SINFONI instrument (Bonnet et al. 2004), installed on the Very Large Telescope UT4 (Yepun) to conduct a spectral analysis of AB Pic b over the 1.1–2.45 μm range. The instrument benefits from the high angular resolution provided by a modified version of the Multi-Applications Curvature Adaptive Optic (AO) system MACAO (Bonnet et al. 2003) and of the integral field spectroscopy offered by SPIFFI (SPectrograph for Infrared Faint Field Imaging, see Eisenhauer et al. 2003). AB Pic b was observed with the J (1.1–1.4 μm) and $H + K$ (1.45–2.45 μm) gratings at resolving powers of 2000 and 1500, respectively (see Table 1). The AO-loop was closed on the bright AB Pic A ($R = 8.61$). The instrument was used with the 25 mas/pixel pre-optic, which limits the field of view (FoV) to $0.8'' \times 0.8''$. Small dithering of the source (8 different positions) increased the FoV up to $1.1''$ and allowed filtering of residual bad pixels. At the end of each observation, the telescope was nodded on the sky. Telluric standard (STD) stars were observed with identical set-ups without dithering right after AB Pic b. Flat fields, darks, arc-lamp, and distortion calibration frames were obtained in the days following the observations.

The whole dataset was reduced using custom *IDL* routines and the SINFONI data reduction pipeline version 1.9.8 (Abuter et al. 2006). Routines were developed to correct raw images from negatives rows created during the bias subtraction (see *The ESO data reduction cookbook*; version 1.0, ESO, 2007) and to suppress an odd even effect affecting slitlet #25. The pipeline carried out cube reconstruction from images corrected from the bias and the odd even effect. Hot and nonlinear pixels were first flagged. The distortion, the wavelength scale, and the slitlet positions were then computed on the entire detector using arc-lamp frames. Slitlet distances were measured with north-south scanning of the detector illuminated with an optical fiber. Object-sky frame pairs were subtracted, flat-fielded and corrected for bad pixels and distortions. Datacubes were finally reconstructed from clean science images and merged into a master cube. Filtering of sky line residuals resulting from sky variation was first done with the pipeline. A second iteration was performed on the slices of each individual datacube before merging then in the final master cube. Finally, an additional routine was implemented to detect and interpolate residual bad pixels.

AB Pic b datacubes did not suffer from the contamination of the nearby AB Pic A but were instead dominated by noise. Atmospheric refraction produces a shift of the source with wavelength in the FoV (from 12.5 to ~ 70 mas). The source was then re-centered slice per slice using polynomial-fit and sub-pixelic shifts with bicubic-spline magnification. The flux of the

¹ Following the definition of the *International Astronomical Union*.

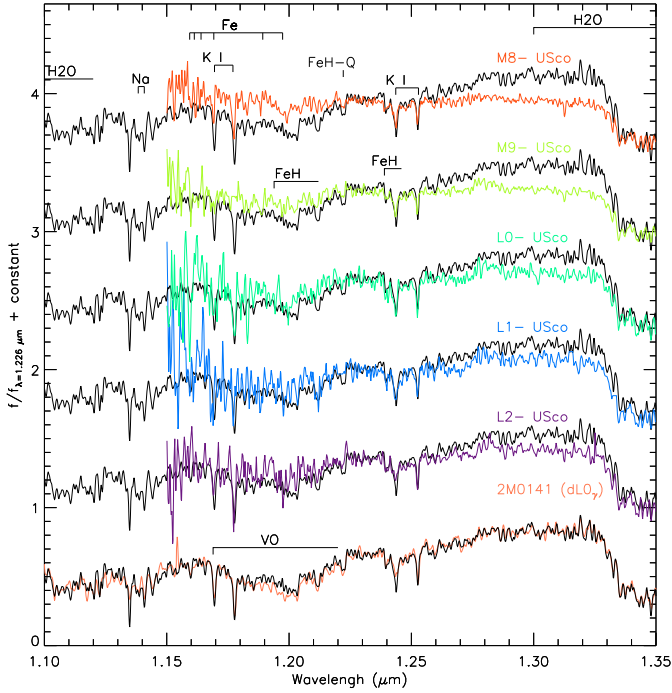


Fig. 1. *J*-band SINFONI spectrum (1.1–1.4 μm) of AB Pic b (black) compared to young (~ 5 Myr) Upper-Sco brown-dwarf spectra (color) over the 1.15–1.35 μm range and to the SINFONI spectrum (salmon-pink) of the young isolated object 2M0141 (classified dL0 $_{\gamma}$). AB Pic b and 2M0141 spectra were convolved with a Gaussian kernel to match the resolution of Upper-Sco spectra ($R = 1400$). χ^2 are minimized for young L1 and L2 dwarfs.

source was then integrated over an aperture minimizing the noise without introducing differential flux losses (radii of 187.5 to 512.5 mas). The STD datacubes were first divided by a black body curve at the T_{eff} of the star, and the flux was collected over the entire FoV. The STD spectra were then corrected from intrinsic features using a Legendre polynomial interpolation over the surrounding continuum. AB Pic b spectra were then divided by STD spectra, normalized, and averaged to form a final spectrum.

3. Spectral analysis

3.1. Empirical comparison

The *J*, *H*, and *K*-band normalized spectra of AB Pic b are presented in Figs. 1–3. The signal-to-noise ratio ranges from 40 in the *H* band to 50 in the *J* and *K* bands. They are compared to young M8–L2 brown dwarfs spectra of Upper Sco (~ 5 Myr) (Lodieu et al. 2008, hereafter L08) at identical resolutions. In addition, *H* and *K*-band spectra are compared to the spectrum of the L4 $^{+1}_{-2}$ companion candidate to 1RXS J160929.1-210524, member of Upper Sco (Lafrenière et al. 2008). In agreement with our expectations, the AB Pic b spectra are typical of young late-M/early-L dwarfs. The triangular shape of the *H*-band (Lucas et al. 2001; Luhman et al. 2004), the bumpy *K*-band, the reduced strength of alkali lines (Na I at 1.138 μm , K I doublets at 1.169/1.177 and 1.243/1.253 μm and the K I line at 1.517 μm), and of FeH absorptions over the *J* and *H* bands (Wallace & Hinkle 2001; Cushing et al. 2003) all results from the intermediate surface gravity of the companion. This is illustrated in Fig. 4, where the *J*-band spectrum of AB Pic b shows intermediate-gravity K I doublets compared to the low and high-gravity spectra of the IO Vir giant star and field dwarfs.

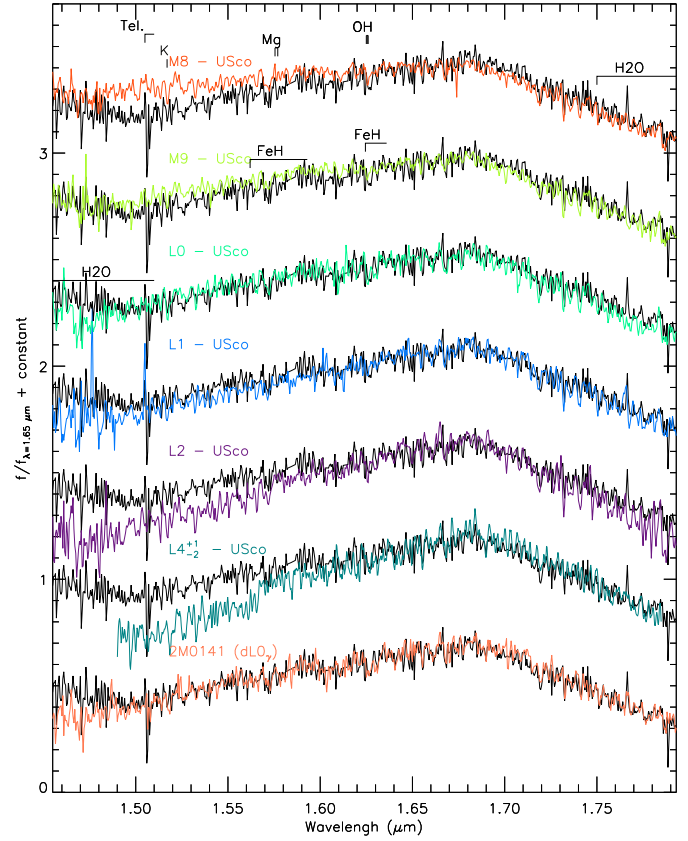


Fig. 2. *H*-band SINFONI spectrum (1.45–1.8 μm) of AB Pic b (black) compared to young (~ 5 Myr) Upper-Sco brown-dwarf spectra (color) over the 1.5–1.8 μm range and to the SINFONI spectrum (salmon-pink) of the young isolated object 2M0141 (classified dL0 $_{\gamma}$). χ^2 are minimized for a young L0 dwarf. The triangular profile of our spectrum results from reduced collision-induced absorption of H $_2$ observed in young objects.

Table 2. Spectral indexes and associated spectral types for AB Pic b.

Index	H $_2$ O $_A$	H $_2$ O-1	H $_2$ O-2	H $_2$ O	K1	K2
Value	0.57	0.61	0.89	1.14	0.1	0.04
Sp. type	L2 \pm 2	L2 \pm 2	L0 \pm 2	M9 \pm 2	L_{pec}	L_{pec}

To assign a spectral type, we used two different approaches. We first compared our spectra to those of young M8–L4 brown dwarfs (from L08 and Lafrenière et al. 2008) classified in the near-infrared. A χ^2 minimization was obtained for young L1 and L2 dwarfs in the *J* band, L0 dwarf in the *H* band and, L0 and L2 dwarfs in the *K* band. L2 and L4 were excluded from the visual comparison of the pseudo-continuum shape in the *H*-band. We also used spectral indexes to measure the depth of water absorptions at 1.34 μm (H $_2$ O $_A$ and H $_2$ O-1; see McLean et al. 2003; Slesnick et al. 2004), 1.5 μm (H $_2$ O, see Allers et al. 2007), and 2.04 μm (H $_2$ O-2, see Slesnick et al. 2004). These absorptions are only slightly sensitive to the age. These indexes confirmed that AB Pic b has a near-infrared spectral type between a L0 and L1 (Table 2). The K1 and K2 indexes measuring the strength of the H $_2$ O band from 2.0 to 2.14 μm , and of the H $_2$ absorption around 2.2 μm respectively (Tokunaga & Kobayashi 1999, hereafter T99) finally discriminated AB Pic b (L_{pec}) from old field dwarfs (see Fig. 4 of T99; computed for young BD and field dwarfs).

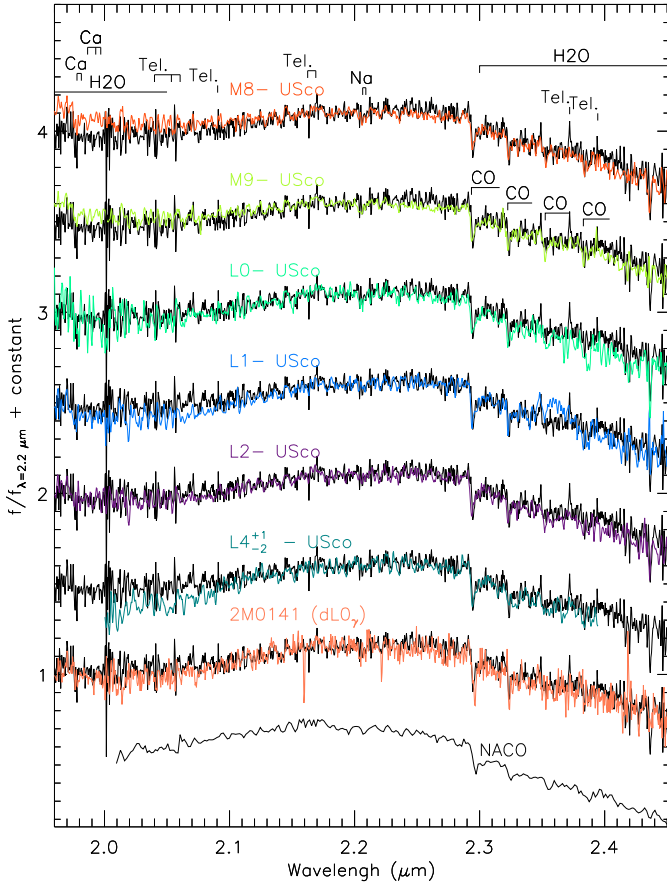


Fig. 3. *K*-band SINFONI spectrum of AB Pic b (black) compared to young (~ 5 Myr) Upper-Sco brown-dwarf spectra (color) and to the young isolated object 2M0141 (classified dL0 $_{\gamma}$). χ^2 are minimized for young L0 and L2 dwarfs. The shape is not reproduced well by old field dwarfs. The low-resolution ($R_{\lambda} = 550$) NACO spectrum is overplotted at the bottom for comparison.

However, near-infrared spectral types are not necessarily consistent with those inferred at optical wavelengths where a homogeneous classification scheme for field and young brown dwarfs exists. We noticed that the normalized spectra of the L08 sample tend to be bluer than those of AB Pic b in the *J* band. AB Pic b normalized *H* + *K* band spectrum also appear over-luminous in the *K* band (or underluminous in the *H*-band). The only exceptions are UScoJ163919-253409 and UScoJ160918-222923 (classified as L1 by L08) for which a good simultaneous fit in the *J* and *H* + *K* bands is achieved. This discrepancy could be related to peculiar dust properties, differences in dust opacities, binarity, or even extinction by a disk (Luhman et al. 2007). However, Herczeg et al. (2009) reveals that the classification of L dwarfs given in L08 could be strongly revised using optical spectra. We then ultimately decided to compare our spectra to those of the young L0 dwarf 2MASS J01415823-4633574 (Kirkpatrick et al. 2006, hereafter K06). This dwarf (hereafter 2M0141) has been classified in the optical following the scheme of Kirkpatrick (2005). The excellent match of our spectrum with that of 2M0141 in the *J*, and *H* + *K* bands (see Figs. 1–3) leads us to assign a final spectral type L0–L1 to AB Pic b.

A T_{eff} -spectral type conversion scales have not been established for young early-L dwarfs yet. However, the Luhman et al. (2003) scale valid for young M dwarfs (~ 2 Myr) gives an upper limit for the effective temperature of 2400 K. L08 give in

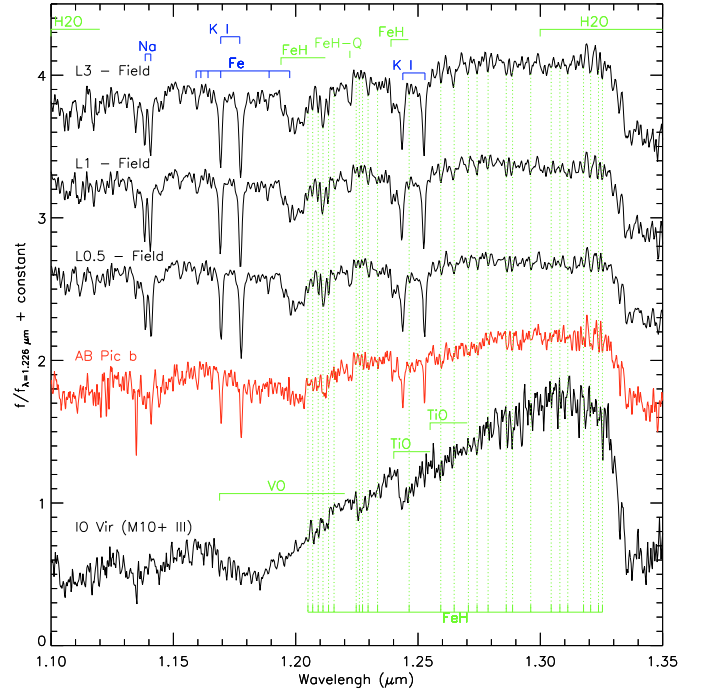


Fig. 4. *J*-band SINFONI spectrum of AB Pic b (red) compared to the spectrum of a late-type M giant (IO Vir) and to field dwarf spectra (Cushing et al. 2005) over the 1.1–1.35 μm range. Atomic features are plotted in blue and molecular absorptions in green.

addition an estimation of $2000 \text{ K} \lesssim T_{\text{eff}} \lesssim 2300 \text{ K}$ for L0 to L1 young brown-dwarfs of the Upper Sco association.

3.2. Comparison to atmosphere grids

We used the AMES–Dusty00 library of synthetic spectra² (Allard et al. 2001) that incorporates formation of dust in the atmosphere for $T_{\text{eff}} \lesssim 2600 \text{ K}$. Spectra were convolved by a Gaussian kernel to match the resolution of SINFONI, interpolated on the AB Pic b wavelength grid, and normalized at 1.226 μm , 1.56 μm , and 2.2 μm in the *J*, *H*, and *K* band. The H₂O absorptions from 1.32 to 1.60 μm and from 1.75 to 2.20 μm are known to be overestimated in the models (Leggett et al. 2001; Lucas et al. 2001; Kirkpatrick et al. 2006). We then compared the AB Pic b spectral continuum to spectral models over the 1.1–1.34 μm zone using a classical, weighted least-square method. The analysis led to $T_{\text{eff}} = 2000 \pm 100 \text{ K}$ and $\log(g) = 4.0 \pm 0.5$ dex. The fit was still visually acceptable for T_{eff} down to 1700 K and up to 2100 K (see Figs. 5 and 6). Comparatively, K06 find similar atmospheric parameters for 2M0141.

The *K*-band was not properly fitted at $T_{\text{eff}} = 2000 \text{ K}$, and higher effective temperatures ($T_{\text{eff}} = 2500 \text{ K}$) could match the observed depth of CO overtones at $\lambda \gtrsim 2.3 \mu\text{m}$ better and the shape of the pseudo-continuum. The case of 2M0141 is likely to be similar (see the lower panel of Fig. 9 of K06). Finally, the *K*-band of AB Pic b was reproduced better at $T_{\text{eff}} = 2000 \text{ K}$ and $\log(g) = 4.0$ dex using the most recent SETTL08 library. This library incorporates an updated bank of molecular opacities (BT), a more realistic mixing length parameter ($\alpha = 2$), and settling and replenishment of the dust in the photosphere.

Finally, the *H*-band is marginally reproduced by AMES–Dusty00 and SETTL08 models. These non-reproducibilities are

² The spectra can be generated on demand on <http://phoenix.ens-lyon.fr/simulator/index.faces>

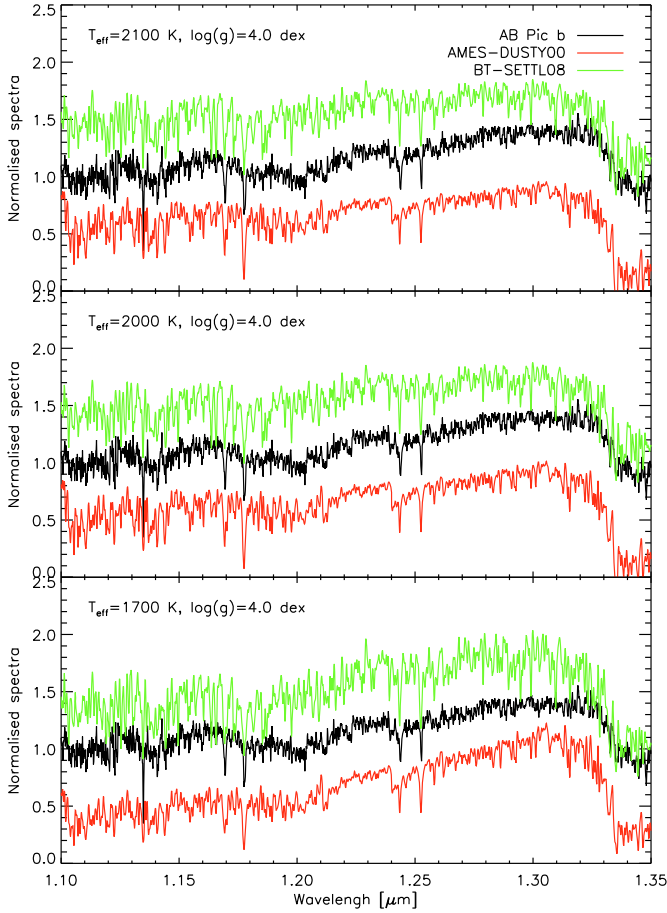


Fig. 5. Comparison of the AB Pic b *J* band spectrum to the synthetic spectra of the AMES-DUSTY00 and SETTL08 libraries at $\log(g) = 4.0$ dex, $[M/H] = 0$ dex, and $T_{\text{eff}} = 1700$ K, 2000 K and 2100 K.

strengthened in SETTL08 spectra by an incorrect representation of the thermal structure of the photosphere. This effect is also responsible for the overestimation of several narrow absorptions in the *J* band (see Fig. 5).

Nordström et al. (2004) reports AB Pic A as a metal poor star with $\text{Fe}/\text{H} = -0.64 \pm 0.12$ dex. However, this estimation relies on a relation based on color indexes that could be biased for very young objects. More recently, Viana Almeida et al. (2009, hereafter V09) have measured spectroscopically a $\text{Fe}/\text{H} = +0.07$ dex. At a distance of ~ 260 AU, one probable formation mechanism for AB Pic b is via a binary-like process, i.e. with initial abundances similar to those of AB Pic A. We then compared our spectrum to SETTL08 models with Fe/H between -0.5 and 0.0 and $T_{\text{eff}} = 2000^{+100}_{-300}$ K to test their influence on our fits. The models indicate that subsolar abundances do not change the *J*-band pseudo-continuum but increase the depth of the K I doublets at $1.169/1.177 \mu\text{m}$ and $1.243/1.253 \mu\text{m}$ (see Fig. 7). The *K*-band shows weaker CO overtones and reduced H_2O absorptions (see Fig. 8). This effect does not affect our T_{eff} estimation but could lead to slightly lower $\log(g)$ estimates. A more extensive analysis of our spectra with dedicated synthetic spectra libraries could add new constraints on individual abundances of AB Pic b.

In conclusion, both AMES-DUSTY00 and SETTL08 libraries yield $T_{\text{eff}} = 2000^{+100}_{-300}$ K and $\log(g) = 4.0 \pm 0.5$ dex for AB Pic b, for solar and subsolar ($\text{Fe}/\text{H} = -0.5$) metallicities. In comparison, Mohanty et al. (2007) (hereafter M07) fit near-infrared colors and absolute photometry of AB Pic b with SETTL05 and

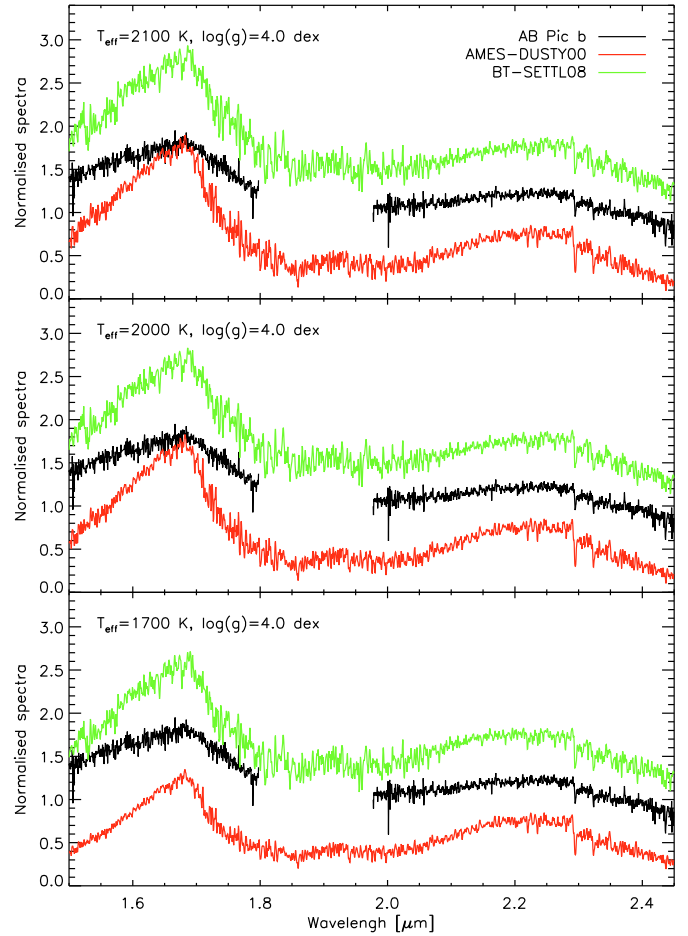


Fig. 6. Comparison of the AB Pic b *H+K* band spectrum to the synthetic spectra of the AMES-DUSTY00 and SETTL08 libraries at $\log(g) = 4.0$, $[M/H] = 0$ dex, and $T_{\text{eff}} = 1700$ K, 2000 K and 2100 K.

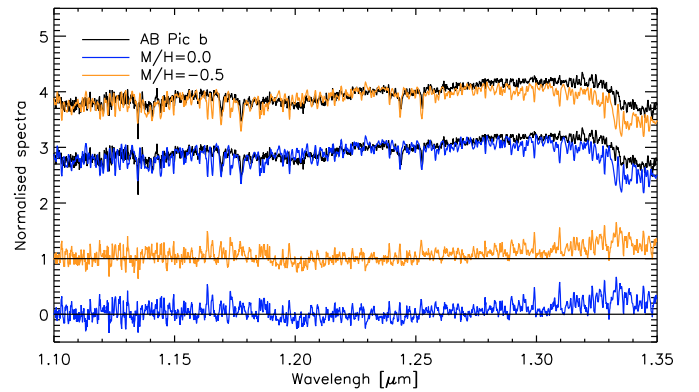


Fig. 7. Comparison of the AB Pic b *J* band spectrum to normalized synthetic spectra (along with residuals) of the SETTL08 library at $\log(g) = 4.0$, $T_{\text{eff}} = 2000$ K, and $-0.5 < [M/H] < 0.0$.

AMES-DUSTY00 models. They find a good match for $T_{\text{eff}} = 1700\text{--}1800$ K and $\log(g) = 4.25$. Similarly, the SETTL08 grid reproduces the observed colors for $T_{\text{eff}} = 1600\text{--}1700$ K and $\log(g) = 4.0\text{--}4.5$. However, the lack of reproducibilities of synthetic spectra in the *H* and *K* bands revealed here shows that near-infrared colors and absolute fluxes should be used with care to infer the properties of young and cool objects.

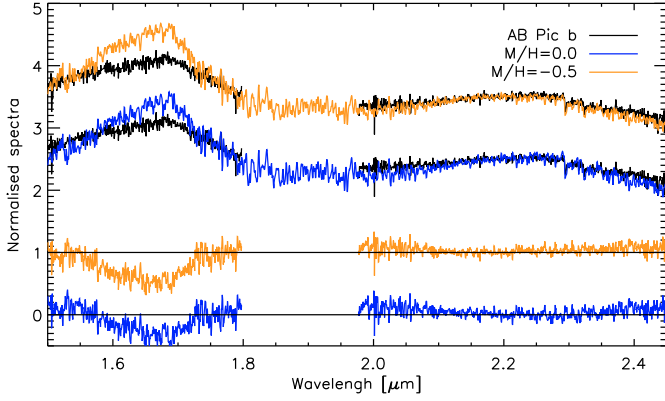


Fig. 8. Same as Fig. 7 but for the $H+K$ band.

4. Radius, mass, and luminosity of AB Pic b

4.1. Evolutionary model predictions

Masses of young substellar companions are mostly derived from evolutionary models predictions (D’Antona & Mazzitelli 1997; Burrows et al. 1997; Baraffe et al. 1998; Chabrier et al. 2000; Baraffe et al. 2003; Saumon & Marley 2008). State of the art models are based on the combination of interior models and atmospheric models necessary to link up the luminosities in observed bands to the mass, radius, effective temperatures, and surface gravities at different ages and metallicities (tracks). From the de-reddened magnitudes and colors in the 2MASS passbands, the AMES–Dusty00 evolutionary models (Chabrier et al. (2000); using AMES–Dusty00 atmospheric models) predict for AB Pic b a mass of $10 M_{\text{Jup}} \leq M \leq 14 M_{\text{Jup}}$ (see Table 3). Using T_{eff} derived from our spectral analysis leads to a similar prediction of $11 M_{\text{Jup}} \leq M \leq 14 M_{\text{Jup}}$. Scarce direct mass measurements of young brown dwarfs and very low-mass stars seem to reveal that models do not achieve a good simultaneous prediction of T_{eff} , luminosities, radii, and masses of young low-mass objects (see Mathieu et al. 2007). Tracks need to be calibrated at young ages and very low masses down to the planetary mass regime where the formation mechanisms could actually play a key role (Marley et al. 2007). One can therefore try to use alternative methods of estimating the mass of substellar companions.

4.2. Alternative estimations

Based on the empirical relations between BC_K and spectral types, the luminosity of the object can be determined independently from evolutionary tracks. In the case of an L0–L1 spectral type, we derived a bolometric correction $\text{BC}_K = 3.24^{+0.18}_{-0.19}$ mag from the relations of Golimowski et al. (2004) valid for field dwarfs. Luminosity, radius, and mass can then be deduced based on T_{eff} and $\log(g)$ derived from our spectral analysis (see the second line in Table 3). The estimated mass agrees with evolutionary model predictions but with much larger uncertainties. However, the assumption of a similar BC_K -SpT relation between young and field dwarfs has never been established and could therefore add systematic errors that are difficult to quantify.

An alternative approach has been introduced by Mohanty et al. (2004, hereafter M04) to estimate the masses, radii, and luminosities of isolated substellar objects of the Upper Sco association. The method is to use the surface flux provided by atmospheric models at the distance of the system. In the specific case of AB Pic b, considering $A_V = 0.27 \pm 0.02$

Table 3. Updated AB Pic b properties.

Method	T_{eff} (K)	$\log(g)$	$\log(L/L_{\odot})$	Radius (R_{Jup})	Mass (M_{Jup})
Evol.	1750^{+100}_{-100}	4.2 ± 0.2	-3.6 ± 0.2	1.5–1.6	10–14
BC_K	2000^{+100}_{-300}	4.0 ± 0.5	-3.7 ± 0.2	$1.22^{+0.70}_{-0.25}$	1–45
$F_{\text{surf}-J}$	2000^{+100}_{-300}	4.0 ± 0.5	$-4.00^{+0.33}_{-0.16}$	$0.81^{+0.83}_{-0.2}$	1–21
$F_{\text{surf}-K}$	2000^{+100}_{-300}	4.0 ± 0.5	$-3.72^{+0.15}_{-0.20}$	$1.13^{+0.38}_{-0.11}$	2–24

(see van Belle & von Braun 2009), the absolute magnitude in K -band can therefore be combined with the surface flux of the AMES–Dusty00 spectra at $T_{\text{eff}} = 2000$ K and $\log(g) = 4.0$ (computed in the 2MASS filters) to determine the companion radius. From the radius and the surface gravity, we can deduce the mass, and considering in addition T_{eff} , we derive the luminosity. All results are reported in Table 3. The same approach can be taken using J -band flux, leading to slightly different values as explained by a non-simultaneous reproducibility of the J and K_s -band surface flux at $T_{\text{eff}} = 2000$ K. This effect has already been noticed in M04 for derivations of the radii, luminosities, and masses from I_C and J magnitudes. In both cases, estimated masses of AB Pic b again agree with evolutionary model predictions within uncertainties. The errors on these parameters results from propagated errors of the atmospheric parameters of our spectral analysis (that make the surface flux vary) and of the absolute photometry. Similar result are derived from the SETTL08 surface fluxes.

Both methods lead to consistent masses, luminosities, surface gravities, and T_{eff} with evolutionary model predictions, but do not allow actually testing and refining them. Our conclusions are very sensitive to the values of T_{eff} and $\log(g)$ inferred from our spectral analysis, hence adequate atmosphere spectral modeling. The strong overprediction of H_2O absorptions that dominate the shape of the near-infrared spectrum of L dwarfs, even for the most recent atmospheric models, and the non-simultaneous reproducibility of the J , H , and K bands both indicate that the comparison of the near-infrared spectra of planetary mass companions to synthetic spectra is not straightforward. It will therefore remain a difficult task for future direct-imaging detection and characterization, which will rely on lower resolution spectra in the near-infrared and similar libraries of synthetic spectra. For planetary mass companions at very wide orbits (no expected contamination from the primary), fitting the spectral energy distribution over a broader spectral range and directly measuring the companion luminosity with combined thermal L - or M -band photometry or spectroscopy would certainly lead to a more robust estimation of mass and radius, as recently obtained by Leggett et al. (2008) in the case of HN Peg B.

5. Conclusions

We obtained high-quality 1.1–2.5 μm medium-resolution spectra of the young very low-mass companion AB Pic b, whose evolutionary models place it on the planet/brown-dwarf boundary. Near-infrared spectra of young M8–L4 dwarfs were compared to the spectrum of AB Pic b using least-square fitting and spectral indexes. They confirmed the youth of the object and allowed refinement of the spectral type estimation of Chauvin et al. (2005b) to L0–L1. Our spectral classification was also confirmed by the excellent match of our spectrum to that of the young L0 field dwarf 2MASS J01415823-4633574 classified in

the visible. A comparison to synthetic spectra enabled us to derive $T_{\text{eff}} = 2000^{+100}_{-300}$ K and $\log(g) = 4.0 \pm 0.5$ compatible with $-0.5 \lesssim \text{Fe}/\text{H} \lesssim 0$. Finally, we used a bolometric correction valid for field L dwarfs and atmospheric models to estimate the mass, the luminosity, and the radii of the companion independently from evolutionary model predictions. The lack of bolometric corrections for young L dwarfs and the large uncertainties related to the determination of the atmospheric parameters do not currently allow the mass of AB Pic b to be refined, as is necessary for making a statement about its status and for testing evolutionary model predictions.

Our study points out the difficulties of inferring young L dwarf companion properties from spectral analysis alone. Alternative methods for the evolutionary models used here rely on uncelebrated relations and atmospheric models. They need to be tested on a wide wavelength range at various gravities (age), effective temperatures, and metallicities. These loopholes will strongly limit the characterization of gaseous planets detected with the upcoming planet finders Gemini/GPI (Macintosh et al. 2006) and VLT/SPHERE (Beuzit et al. 2006, 2008). In that perspective, the XSHOOTER instrument at VLT will help acquiring simultaneous spectra over $0.3\text{--}2.5 \mu\text{m}$ to robustly constrain T_{eff} , $\log(g)$, metallicity, and the luminosity of isolated and wide companion members of young nearby associations and star-forming regions down to the planetary mass regime. The comparison of the observed luminosity to predictions of evolutionary models will also provide a crucial constraint on evolutionary models at young ages and planetary masses, and could also clarify the role of formation mechanisms in this mass range.

Acknowledgements. We are very grateful to the anonymous referee for the constructive review that greatly improved our initial manuscript. We thank the ESO Paranal staff for performing the service-mode observations. We also acknowledge partial financial support from the *Agence Nationale de la Recherche* and the *Programmes Nationaux de Planétologie et de Physique Stellaire* (PNP & PNPS), in France. We are grateful to Andreas Seifahrt, David Lafrenière, and Nicolas Lodieu for providing their spectra. Finally, this work would have not been possible without the NIRSPEC (<http://www.astro.ucla.edu/~mclean/BDSSArchive/>), IRTF (http://irtfweb.ifa.hawaii.edu/~spex/IRTF_Spectral_Library/), and SpecX (<http://www.browndwarfs.org/spexprism>) libraries maintained by Ian S. McLean, Michael C. Cushing, John T. Rayner, and Adam Burgasser.

References

- Abuter, R., Schreiber, J., Eisenhauer, F., et al. 2006, *New Astron. Rev.*, 50, 398
Allard, F., Hauschildt, P. H., Alexander, D. R., Tamanai, A., & Schweitzer, A. 2001, *ApJ*, 556, 357
Allers, K. N., Jaffe, D. T., Luhman, K. L., et al. 2007, *ApJ*, 657, 511
Baraffe, I., Chabrier, G., Allard, F., & Hauschildt, P. H. 1998, *A&A*, 337, 403
Baraffe, I., Chabrier, G., Barman, T. S., Allard, F., & Hauschildt, P. H. 2003, *A&A*, 402, 701
Barnes, J. R., Barman, T. S., Jones, H. R. A., et al. 2009, in *American Institute of Physics Conference Series*, ed. E. Stempels, 1094, 417
Beuzit, J.-L., Feldt, M., Dohlen, K., et al. 2006, *The Messenger*, 125, 29
Beuzit, J.-L., Feldt, M., Dohlen, K., et al. 2008, *SPIE Conf. Ser.*, 7014
Bonnet, H., Abuter, R., Baker, A., et al. 2004, *The Messenger*, 117, 17
Bonnet, H., Ströbele, S., Biancat-Marchet, F., et al. 2003, in *Adaptive Optical System Technologies II*, ed. P. L. Wizinowich, D. Bonaccini, *Proc. SPIE*, 4839, 329
Burrows, A., Marley, M., Hubbard, W. B., et al. 1997, *ApJ*, 491, 856
Chabrier, G., Baraffe, I., Allard, F., & Hauschildt, P. 2000, *ApJ*, 542, 464
Chauvin, G., Thomson, M., Dumas, C., et al. 2003, *A&A*, 404, 157
Chauvin, G., Lagrange, A.-M., Dumas, C., et al. 2004, *A&A*, 425, L29
Chauvin, G., Lagrange, A.-M., Dumas, C., et al. 2005a, *A&A*, 438, L25
Chauvin, G., Lagrange, A.-M., Zuckerman, B., et al. 2005b, *A&A*, 438, L29
Chauvin, G., Lagrange, A.-M., Bonavita, M.-A., et al. 2009, *A&A*, 509, A52
Cushing, M. C., Rayner, J. T., Davis, S. P., & Vacca, W. D. 2003, *ApJ*, 582, 1066
Cushing, M. C., Rayner, J. T., & Vacca, W. D. 2005, *ApJ*, 623, 1115
D'Antona, F., & Mazzitelli, I. 1997, *Mem. Soc. Astron. Ital.*, 68, 807
Eisenhauer, F., Abuter, R., Bickert, K., et al. 2003, in *SPIE Conf. Ser.* 4841, ed. M. Iye & A. F. M. Moorwood, 1548
Golimowski, D. A., Leggett, S. K., Marley, M. S., et al. 2004, *AJ*, 127, 3516
Gorlova, N. I., Meyer, M. R., Rieke, G. H., & Liebert, J. 2003, *ApJ*, 593, 1074
Herczeg, G. J., Cruz, K. L., & Hillenbrand, L. A. 2009, *ApJ*, 696, 1589
Kastner, J. H., Zuckerman, B., Weintraub, D. A., & Forveille, T. 1997, *Science*, 277, 67
Kirkpatrick, J. D. 2005, *ARA&A*, 43, 195
Kirkpatrick, J. D., Barman, T. S., Burgasser, A. J., et al. 2006, *ApJ*, 639, 1120
Lafrenière, D., Jayawardhana, R., & van Kerkwijk, M. H. 2008, *ApJL*, 689, L153
Leggett, S. K., Allard, F., Geballe, T. R., Hauschildt, P. H., & Schweitzer, A. 2001, *ApJ*, 548, 908
Leggett, S. K., Saumon, D., Albert, L., et al. 2008, *ApJ*, 682, 1256
Lodieu, N., Hambly, N. C., Jameson, R. F., & Hodgkin, S. T. 2008, *MNRAS*, 383, 1385
Lowrance, P. J., McCarthy, C., Becklin, E. E., et al. 1999, *ApJ*, 512, L69
Lowrance, P. J., Schneider, G., Kirkpatrick, J. D., et al. 2000, *ApJ*, 541, 390
Lucas, P. W., Roche, P. F., Allard, F., & Hauschildt, P. H. 2001, *MNRAS*, 326, 695
Luhman, K. L., Stauffer, J. R., Muench, A. A., et al. 2003, *ApJ*, 593, 1093
Luhman, K. L., Peterson, D. E., & Megeath, S. T. 2004, *ApJ*, 617, 565
Luhman, K. L., Adame, L., D'Alessio, P., et al. 2007, *ApJ*, 666, 1219
Macintosh, B., Graham, J., Palmer, D., et al. 2006, *SPIE Conf. Ser.* 6272
Makarov, V. V. 2007, *ApJS*, 169, 105
Marley, M. S., Fortney, J. J., Hubickyj, O., Bodenheimer, P., & Lissauer, J. J. 2007, *ApJ*, 655, 541
Mathieu, R. D., Baraffe, I., Simon, M., Stassun, K. G., & White, R. 2007, in *Protostars and Planets V*, ed. B. Reipurth, D. Jewitt, & K. Keil, 411
McLean, I. S., McGovern, M. R., Burgasser, A. J., et al. 2003, *ApJ*, 596, 561
Mentuch, E., Brandeker, A., van Kerkwijk, M. H., Jayawardhana, R., & Hauschildt, P. H. 2008, *ApJ*, 689, 1127
Mohanty, S., Basri, G., Jayawardhana, R., et al. 2004, *ApJ*, 609, 854
Mohanty, S., Jayawardhana, R., Huélamo, N., & Mamajek, E. 2007, *ApJ*, 657, 1064
Nordström, B., Mayor, M., Andersen, J., et al. 2004, *A&A*, 418, 989
Perryman, M. A. C., Lindgren, L., Kovalevsky, J., et al. 1997, *A&A*, 323, L49
Saumon, D., & Marley, M. S. 2008, *ApJ*, 689, 1327
Scholz, A., Coffey, J., Brandeker, A., & Jayawardhana, R. 2007, *ApJ*, 662, 1254
Slesnick, C. L., Hillenbrand, L. A., & Carpenter, J. M. 2004, *ApJ*, 610, 1045
Smith, B. A., & Terrile, R. J. 1984, *Science*, 226, 1421
Song, I., Zuckerman, B., & Bessell, M. S. 2003, *ApJ*, 599, 342
Stelzer, B., & Neuhäuser, R. 2000, *A&A*, 361, 581
Tinetti, G., & Beaulieu, J.-P. 2009, in *IAU Symposium*, 253, 231
Tokunaga, A. T., & Kobayashi, N. 1999, *AJ*, 117, 1010
Torres, C. A. O., da Silva, L., Quast, G. R., de la Reza, R., & Jilinski, E. 2000, *AJ*, 120, 1410
Torres, C. A. O., Quast, G. R., de La Reza, R., da Silva, L., & Melo, C. H. F. 2001, in *Young Stars Near Earth: Progress and Prospects*, ed. R. Jayawardhana & T. Greene, *ASP Conf. Ser.*, 244, 43
Torres, C. A. O., Quast, G. R., da Silva, L., et al. 2006, *A&A*, 460, 695
Torres, C. A. O., Quast, G. R., Melo, C. H. F., & Sterzik, M. F. 2008, *Young Nearby Loose Associations*, ed. B. Reipurth, 757
van Belle, G. T., & von Braun, K. 2009, *ApJ*, 694, 1085
Viana Almeida, P., Santos, N. C., Melo, C., et al. 2009, *A&A*, 501, 965
Vidal-Madjar, A., Désert, J.-M., Lecavelier des Etangs, A., et al. 2004, *ApJL*, 604, L69
Wallace, L., & Hinkle, K. 2001, *ApJ*, 559, 424
Zuckerman, B., & Song, I. 2004, *ARA&A*, 42, 685
Zuckerman, B., & Webb, R. A. 2000, *ApJ*, 535, 959
Zuckerman, B., Song, I., & Webb, R. A. 2001, *ApJ*, 559, 388